

# An Unusual Iron Site in Iron-Doped Zinc Oxide

Ruiping Wang and Arthur W. Sleight

*Department of Chemistry, Oregon State University, Corvallis, Oregon 97331-4003*

and

M. A. Subramanian

*Central Research & Development Department, E. I. du Pont de Nemours & Co., Experimental Station, Wilmington, Delaware 19880-0328*

Received November 22, 1995; in revised form April 28, 1996; accepted June 3, 1996

Both divalent and trivalent iron have been substituted into the zinc oxide lattice at levels up to about 2.5 atomic percent. Using enriched  $^{57}\text{Fe}$ , Mössbauer studies indicate that either  $\text{Fe}^{2+}$  or  $\text{Fe}^{3+}$  may substitute for  $\text{Zn}^{2+}$  at its normal lattice site. One spectrum indicative of  $\text{Fe}^{3+}$  is observed when iron is substituted into zinc oxide under oxidizing conditions. However, two distinct spectra are found for  $\text{Fe}^{2+}$  when iron is substituted into zinc oxide under reducing conditions. The quadrupole splitting of one of these  $\text{Fe}^{2+}$  spectra shows an exceptionally high temperature dependence. © 1996 Academic Press, Inc.

## INTRODUCTION

Zinc oxide based materials have many interesting and useful properties. Applications of such materials are especially attractive on consideration of the low cost and lack of toxicity of zinc oxide. Important uses of zinc oxide include catalysts, luminescent materials, fungicides, surface acoustic wave devices, varistors, and transparent conductors. We have been preparing and studying zinc oxide powders (1, 2) and films (3) that have been doped with elements such as B, Al, Ga, In, Ge, and Na. Local probes used to investigate the environment of the dopant were time differential perturbed angular correlation (TDPAC) for In and NMR for Al, Ga, and Na. We believed that our understanding of zinc oxide might be further enhanced by using  $^{57}\text{Fe}$  Mössbauer to study the environment of iron doped into zinc oxide.

Apparently, there has been only one previous study (4) on the solubility of iron in zinc oxide. That study is of somewhat limited value because the oxygen fugacity during synthesis was not reported. However, based on optical spectra, the authors concluded that their samples contained only divalent iron. Very low levels of  $\text{Fe}^{3+}$  in zinc oxide have been studied by ESR and by emission, excitation, and magneto-optical spectroscopy (5).

## EXPERIMENTAL

Iron-doped ZnO powders were prepared by mixing Fe metal (99.9+%, EM Science) with reagent grade ZnO (99.7+%, Aldrich) powders. The mixtures were ground thoroughly using an agate mortar and pestle before being sealed in predried silica tubes. All tubes were evacuated to ~50–100 mTorr prior to sealing. The tubes were then heated at 1200°C for 10 hours with heating and cooling rates of 5°C/min. The starting Fe-to-ZnO atomic mixing ratios ranged from 1/1000 to 5/100. Iron-doped ZnO samples used in the  $^{57}\text{Fe}$ -Mössbauer experiments were prepared the same way except that iron powder enriched with 95.3 at.%  $^{57}\text{Fe}$  was used.

X-ray diffraction data were obtained using a Siemens D-5000 diffractometer. Electron microprobe analysis (EMPA) was used to determine the actual iron doping concentration. The conductivities of Fe-doped ZnO powders were measured at various applied pressures at room temperature. The measurement method is described in detail elsewhere (1). Iodimetric titration (2) was used to assess the degree of reduction of the samples. Mössbauer spectroscopy data were obtained from Mössbauer Consultants, Inc. (Burlington, MA).

## RESULTS

Iron-doped ZnO samples prepared under vacuum from zinc oxide and iron metal were green in color, and this color intensified as the iron content increased. The green color changes to red when the samples are heated in air at 800°C or above for a few hours. X-ray diffraction powder data showed the usual hexagonal zinc oxide pattern with no detectable change in the unit cell dimensions for any of our samples. No second phases were detected by X-ray diffraction when the iron doping level was less than 3%. At higher levels, both  $\text{ZnFe}_2\text{O}_4$  and Fe metal were de-

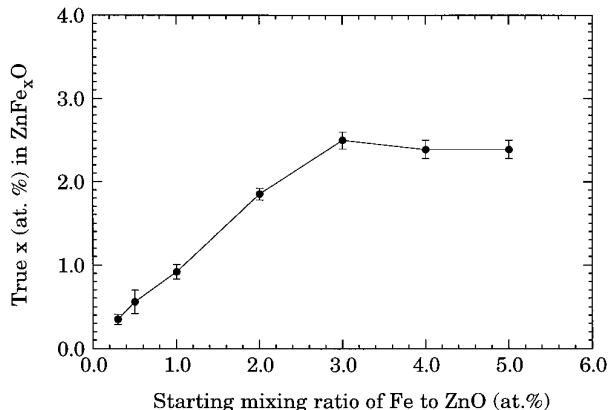


FIG. 1. EMPA analysis of true doping for Fe-doped ZnO.

tected. The lack of phase purity in this case was also apparent from SEM and EMPA studies. The doped zinc oxide particles were  $\sim 20 \mu\text{m}$  in diameter, but additional iron-rich smaller particles were observed at the doping levels where second phases were present.

The conductivities of Fe-doped ZnO powders prepared under reducing conditions were measured at various applied pressures and found to increase with applied pressure. This increase is at least partly due to an increase in the powder density. The measured conductivities did not change as a function of iron doping. In all cases, including undoped zinc oxide treated in the same way, the conductivity measured at a pressure of four tons/cm<sup>2</sup> was  $0.3(\pm 0.1) \Omega^{-1}\text{cm}^{-1}$ . Even though the conductivity was unchanged with doping, EMPA showed as much as 2.5 at.% Fe doping in ZnO under our conditions (Fig. 1). Iodimetric titration results were essentially the same for undoped zinc oxide and zinc oxide doped with iron. This is consistent with the fact that iron doping of zinc oxide does not cause an increase in electrical conductivity.

Samples for Mössbauer spectroscopy were prepared at iron doping levels of 0.5, 1, and 2 at.% in sealed silica tubes. A 1 at.% Fe-doped sample was also prepared in air. Figure 2 shows the Mössbauer spectra of a 1 at.% Fe-doped ZnO sample prepared in a sealed silica tube. At low temperatures, two different types of iron are apparent. The isomer shifts of both types of iron were essentially the same [ $\sim 0.9(1) \text{ mm/s}$ ], indicating that both types of iron were Fe<sup>2+</sup> tetrahedrally coordinated to oxygen (6). The quadrupole splitting for one type of iron (at site A) changed very little as the temperature was increased to room temperature (Fig. 3). However, the quadrupole splitting for the other type of iron (at site B) decreased dramatically with increasing temperature (Fig. 3) until at room temperature the quadrupole splittings for the two types of iron have become indistinguishable (Fig. 2).

A completely different <sup>57</sup>Fe Mössbauer spectrum is observed for samples of iron-doped zinc oxide prepared in air. In this case, a pair of broad peaks (linewidth of 0.7(1) mm/s for each peak of the doublet) is found with an isomer shift of 0.28 mm/s and a quadrupole splitting of 0.60 mm/s at room temperature. At 77 K, the isomer shift is 0.39 mm/s and the quadrupole splitting is 0.64 mm/s. This is consistent with iron being Fe<sup>3+</sup> occupying a tetrahedral site in the ZnO lattice. There is no suggestion of any other iron site at any temperature.

## DISCUSSION

Zinc oxide can become a good *n*-type conductor when doped with B, Al, Ga, In, Si, or Ge. A characteristic of all

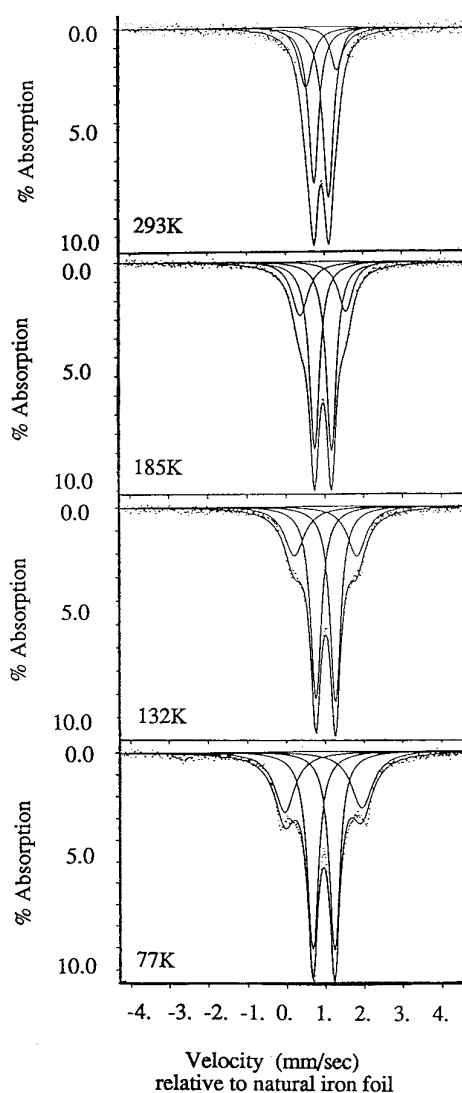


FIG. 2. Mössbauer spectra of 1 at.% Fe-doped ZnO at different temperatures.

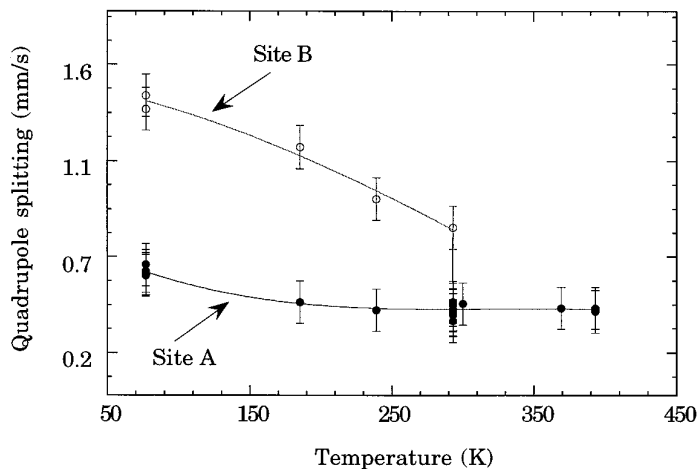


FIG. 3. The temperature dependence of the quadrupole splitting of sites A and B. The solid curve for B site is the fitted curve and that for A site is a guide to the eye only.

of these dopants is the availability of a very stable oxidation state higher than two. When these dopants substitute for  $\text{Zn}^{2+}$  in the zinc oxide lattice, they can produce free carriers,  $\text{Zn}_{1-x}\text{Ga}_x^{3+}\text{O}^{2-}\cdot xe^-$ , for example. This carrier is delocalized in the  $4s$  band, and good conductivity results even for very small carrier concentrations. One might expect an analogous situation for iron-doped zinc oxide, that is,  $\text{Zn}_{1-x}\text{Fe}_x^{3+}\text{O}^{2-}\cdot xe^-$ . If this occurred, high conductivity would be expected as zinc oxide was doped with iron. The lack of such enhanced conductivity suggests that the hypothetical free electron is trapped by  $\text{Fe}^{3+}$ . Thus, the iron substitution for  $\text{Zn}^{2+}$  in zinc oxide should be represented as  $\text{Zn}_{1-x}\text{Fe}_x^{2+}\text{O}^{2-}$ , and no free electrons result from iron doping. Iodimetric titrations readily detect the electrons doped into zinc oxide (1, 2), and our titrations show that no such electrons are produced with iron doping into zinc oxide. Furthermore, our  $^{57}\text{Fe}$  Mössbauer studies on our  $\text{ZnO}:\text{Fe}$  samples prepared under reducing conditions show that essentially all iron is divalent and is on tetrahedral sites.

When  $\text{Fe}^{2+}$  is substituted into zinc oxide, two distinctly different iron sites were always observed. Both have an isomer shift indicative of tetrahedral divalent iron. One site has a small quadrupole splitting which shows very little temperature dependence. The other site shows an unusually large increase in quadrupole splitting as the temperature decreases from room temperature. Such unusual temperature dependence of the quadrupole splitting has been noted (7, 8) for tetrahedral divalent iron in compounds of the type  $R_2\text{FeX}_4$  where  $X$  may be  $\text{Cl}^-$ ,  $\text{Br}^-$ ,  $\text{NCS}^-$ , or  $\text{NCS}_e^-$  and  $R$  may be  $\text{NMe}_4^+$ ,  $\text{NEt}_4^+$ , etc. This temperature dependence is attributed to a distortion of the tetrahedral symmetry which lifts the degeneracy

of the  $e_g$  levels. The tetrahedral site in the zinc oxide structure does not possess true tetrahedral symmetry. Thus, it is a possible candidate for such an effect. However, if the  $\text{Fe}^{2+}$  with the large temperature dependence of the quadrupole splitting is  $\text{Fe}^{2+}$  on a normal  $\text{Zn}^{2+}$  lattice site, this would still leave unanswered the question of the site occupied by  $\text{Fe}^{2+}$  showing a more normal, small temperature dependence of the quadrupole splitting. One of the two iron sites might be the interstitial tetrahedral site, but this would require an unreasonably short  $\text{Zn}^{2+}-\text{Fe}^{2+}$  distance of 1.5 Å before lattice relaxation. The unusual  $\text{Fe}^{2+}$  site would appear to be related to a In site observed by  $^{111}\text{In}$  TDPAC studies of zinc oxide (2).

Time differential perturbed angular correlation studies (2, 9) using a  $^{111}\text{In}$  probe also show two sites in zinc oxide prepared under reducing conditions. One of these sites has an unusually large temperature dependence for the electric field gradient (efg). This unusually large temperature dependence can be fit to a  $T^{3/2}$  function, and we find that such a function also works well for fitting the large temperature dependence of the quadrupole splitting of the iron at site B in zinc oxide. The fitted curve in Fig. 3 is  $\Delta_2 = \Delta_{20} (1-BT^{3/2})$ , where  $\Delta_{20} = 1.47$  mm/s and  $B = 9 \times 10^{-5}$ . Zinc oxide apparently has a range of composition from about  $\text{Zn}_{1.000}\text{O}$  to  $\text{Zn}_{1.0003}\text{O}$ . The excess zinc is commonly assumed to occupy an interstitial site. TDPAC measurements (2) using a  $^{111}\text{In}$  probe show only one site when the Zn-to-O ratio is close to one, and this site has axial symmetry as expected for In on a normal  $\text{Zn}^{2+}$  lattice site. The second site appears only when samples are prepared under reducing conditions. This site lacks axial symmetry, and it intensifies as the Zn-to-O ratio increases. This is the site which shows an unusually high temperature dependence of the efg. It has been suggested that this unusual temperature dependence is caused by a nearby zinc interstitial which is rattling due to the large volume of the site (2). It seems likely that the site producing the highly temperature-dependent efg is the same for the  $^{57}\text{Fe}$  and  $^{111}\text{In}$  probes. However, it does not seem likely that the unusual  $\text{Fe}^{2+}$  site is the result of a nearby Zn interstitial because the concentration of the unusual site is orders of magnitude larger than the maximum concentration of interstitial Zn in  $\text{Zn}_{1+x}\text{O}$ . Conceivably, doping of zinc oxide with  $\text{Fe}^{2+}$  could drastically increase the concentration of Zn interstitials, but this is inconsistent with our iodimetric titrations. We thus conclude that one of the two  $\text{Fe}^{2+}$  sites in  $\text{Fe}^{2+}$ -doped zinc oxide is a normal Zn lattice site and the other is related to an unknown defect. Extended defects are well known to occur in zinc oxide, but they have not been well characterized. One indication of the ease of formation of defects in zinc oxide is the observation (10) that attempts to grind a single crystal to spherical shape led

to diffraction effects caused by damage to the crystal. We thus conclude that the unusual site for  $\text{Fe}^{2+}$  in zinc oxide is likely probing an extended defect, not simply a point defect such as a zinc interstitial. This means that the interpretation which has been offered (2, 9) for the second site observed by  $^{111}\text{In}$  TDPAC studies is likely not correct. It is more likely that this site is related to the same extended defect causing the unusual  $\text{Fe}^{2+}$  site in zinc oxide. This site becomes more prominent when zinc oxide is reduced. Further studies are required to define the defect involved.

Our Mössbauer results show only one type of iron site when  $\text{Fe}^{3+}$  is substituted into zinc oxide. Because this is a trivalent cation on a site for a divalent cation, there must be compensating defects to maintain charge neutrality. These compensating defects could be oxygen interstitials or cation vacancies. The behavior of the  $\text{ZnO}:\text{Fe}^{3+}$  system differs then from that of the  $\text{ZnO}:\text{Ga}^{3+}$  system where both conducting  $\text{Zn}_{1-x}^{2+}\text{Ga}_x^{3+}\text{O}_{1+\frac{y}{2}}$  phases and insulating  $\text{Zn}_{1-y}\text{Ga}_y\text{O}_{1+\frac{y}{2}}$  phases may be prepared (2). In the

$\text{ZnO}:\text{Fe}^{3+}$  system, only insulating  $\text{Zn}_{1-y}\text{Fe}_y\text{O}_{1+\frac{y}{2}}$  phases could be prepared.

## REFERENCES

1. R. P. Wang, A. W. Sleight, and D. Cleary, *Chem. Mater.* **8**, 433 (1996).
2. R. P. Wang, A. W. Sleight, R. Platzter, and J. A. Gardner, *J. Solid State Chem.* **122**, 166 (1996).
3. R. P. Wang, L. L. H. King, and A. W. Sleight, *J. Mater. Res.*, **11**, 1659–1664 (1996).
4. C. H. Bates, W. B. White, and R. Roy, *J. Inorg. Nucl. Chem.* **28**, 397–405 (1966).
5. R. Heitz, A. Hoffmann, and I. Broser, *Phys. Rev. B* **45**(16), 8977–8988 (1992).
6. N. N. Greenwood and T. C. Gibb, “Mössbauer Spectroscopy.” Chapman & Hall, London/New York, 1971.
7. P. R. Edwards, C. E. Johnson, and R. J. P. William, *J. Chem. Phys.* **47**(6), 2074–2082 (1967).
8. T. C. Gibb and N. N. Greenwood, *J. Chem. Soc.*, 6989 (1965).
9. H. Wolf, S. Deubler, D. Forkel, H. Foettinger, M. Iwatschenko-Borho, F. Meyer, M. Renn, W. Witthuhn, and R. Helbig, *Mater. Sci. Forum* **10–12**, 863–868 (1986).
10. H. Sawada, R. Wang, and A. W. Sleight, *J. Solid State Chem.* **122**, 128 (1996).